



Original Article

Protective Effects of *Nigella Sativa* Against Acrylamide-induced Toxicity in Submandibular Salivary Glands of Albino Rats



Salma Awad Taghyan^{1*}, Elham Fathy Mahmoud², Rasha Mohamed Taha², Mohamed Shamel¹

1. Department of Oral Biology, Faculty of Dentistry, The British University in Egypt, Cairo, Egypt.

2. Department of Oral Biology, Faculty of Dentistry, Suez Canal University, Ismailia, Egypt.



How to cite this article Taghyan SA, Mahmoud EF, Taha RM, Shamel M. Shamel. Protective Effects of *Nigella Sativa* Against Acrylamide-induced Toxicity in Submandibular Salivary Glands of Albino Rats. *Archives of Razi Institute Journal*. 2025; 80(5):1209-1216. <https://doi.org/10.32598/ARI.80.5.3494>

doi <https://doi.org/10.32598/ARI.80.5.3494>

Article info:

Received: 22 Apr 2025

Accepted: 18 Jun 2025

Published: 01 Sep 2025

Keywords:

Salivary glands, Acrylamide, *Nigella sativa*, Oxidative stress

ABSTRACT

Introduction: Acrylamide (AA) is a chemical compound that poses a major public health concern. This study aimed to evaluate the protective effect of *Nigella sativa* (NS) oil against AA-induced toxicity on the submandibular salivary glands (SMGs) of Albino rats.

Materials & Methods: Thirty male albino rats weighing 150–200 g were equally and randomly divided into some groups: Control group received normal saline vehicle daily via oral gavage for 30 days, AA group received 15 mg/kg body weight of AA dissolved in 0.2 mL saline solution daily via oral gavage for 30 days. NS group received 15 mg/kg body weight (bw) of AA combined with 1 mL/kg bw of NS oil daily via oral gavage for 30 days. At the end of the experiment, rats were euthanized, and SMGs were dissected for histological evaluation, including hematoxylin and eosin staining (H&E) and immunohistochemistry for inducible nitric oxide synthase (iNOS), as well as analysis for heme oxygenase-1 (*HO-1*) expression using real-time polymerase chain reaction (RT-qPCR).

Results: The acinar and ductal cells of SMG of the AA group showed signs of degeneration and toxicity in the form of ill-defined outlines, pyknotic and crescent-shaped nuclei with different-sized cytoplasmic vacuolations. These changes were statistically significant with increased iNOS immunoreexpression and *HO-1* gene expression ($P < 0.0001$). Administration of NS alleviated the toxic effect, downregulating both iNOS and *HO-1* gene expression. The study revealed a significant cytotoxic effect of AA on SMGs of albino rats ($P < 0.05$), presumably by the generation of oxidative stresses and mitochondrial dysfunction.

Conclusion: NS effectively mitigated these toxic effects, suggesting its potential as a natural antioxidant.

* Corresponding Author:

Salma Awad Taghyan, Assistant Professor.

Address: Department of Oral Biology, Faculty of Dentistry, The British University in Egypt, Cairo, Egypt.

Tel: +20 (114) 5082680

E-mail: sal-ma.taghyan@bue.edu.eg



Copyright © 2025 The Author(s);
This work is licensed under a Creative Commons Attribution-NonCommercial 4.0 International license (<https://creativecommons.org/licenses/by-nc/4.0/>).
Noncommercial uses of the work are permitted, provided the original work is properly cited.

1. Introduction

Acrylamide, or acrylamide (AA), is a solid, odorless, water-soluble compound appearing as white crystals with high chemical activity [1]. AA is widely used in chemical industries such as mining, paper production, cosmetics, textiles, and wastewater treatment, and is considered the foundation for the polymer polyacrylamide [2]. Various levels of AA have been reported in many dietary products, particularly fried and baked foods processed at high temperatures. AA is formed as a by-product of deep frying or cooking of any carbohydrate-rich foods at high temperatures ($>120^{\circ}\text{C}$). It has been described as a cooking-associated carcinogen due to its spontaneous formation during the cooking process, making it a significant public health concern [1]. AA is quickly absorbed through the gastrointestinal system and then distributed to other parts of the body via the bloodstream [2]. In the liver, AA is detoxified by combining with glutathione (GSH), catalyzed by GSH S-transferase (GST). This process results in the formation of N-acetyl-S-cysteine, which is then broken down and eliminated through urine. However, this detoxification process reduces GSH levels, leading to decreased antioxidant capacity and increased oxidative stress. Additionally, AA can be transformed by the cytochrome CYP2E1 enzyme to produce glycidamide (GA), a compound associated with AA's harmful and cancer-causing properties. The interaction between oxidative stress and GA production worsens the damaging effects of AA, including its mutagenic and carcinogenic properties [3].

Several studies indicated that AA exposure can produce neurotoxicity, hepatotoxicity, nephrotoxicity, and reproductive toxicity [1, 4]. Moreover, numerous studies have evaluated the toxic effect of AA on different oral tissues, including salivary glands, tongue, and soft palate [5, 6]. Considering the possibility of extensive oxidative stress and genotoxicity caused by AA, investigating preventative measures is essential. One such measure could be using *Nigella Sativa* (NS), an herbaceous plant traditionally utilized for its medicinal properties. NS treats different conditions like asthma, headache, dizziness, hypertension, inflammation, cough, bronchitis, diabetes, eczema, fever, and gastrointestinal disturbances [7]. Notably, NS oil is recognized as a powerful antioxidant, anti-inflammatory, immunostimulatory, and anti-apoptotic agent. These properties position NS as a promising candidate for mitigating cellular damage caused by oxidative stress, particularly in the context of exposure to food toxins like AA [8]. NS oil and its active constituents, thymoquinones, can decrease oxidative stress levels while upregulating GSH and other antioxidant enzymes such as catalase and superoxide dismutase (SOD) [7, 8].

2. Materials and Methods

2.1. Animals

This study received ethical approval from the Faculty of Dentistry, Suez Canal University. Sample size calculation was performed using G*Power software, version 3.1.9.2 (University Kiel, Germany). The effect size was 0.95 using α level of 0.05 and β level of 0.05, i.e. power=95%; the estimated sample size (n) was a total of 30 rats [9]. Thirty male Albino rats weighing 150–200 g were housed in a sterile, controlled environment (temperature $25\pm 2^{\circ}\text{C}$ and 12-hour dark/light cycles) and fed with a standard laboratory diet and tap water during the study. The rats were kept in individual cages, 5 rats per cage. The size of the cage was 20 cm in width and 40 cm in length. Following an adaptation period of 1 week, the rats were equally and randomly divided into three groups (n=10) as follows:

Control group received normal saline vehicle daily via oral gavage for 30 days.

AA group: Received 15 mg/kg body weight (bw) of AA (Advent Chembio Private Limited Company, Navi Mumbai, India (CAS No. 79-06-1) dissolved in 0.2 mL saline solution daily via oral gavage for 30 days.

AA+NS group received 15 mg/kg bw of AA dissolved in 0.2 mL saline solution, and 1 mL/kg bw of NS oil (Imtenan Health shop company, Obour City, Cairo, Egypt) after AA administration, daily via oral gavage for 30 days [10].

2.2. Histological and immunohistochemical (IHC) procedures

Following the experiment period, rats were sacrificed via an extra dose of anesthesia. All rats' major SMGs were excised. Half the specimens were fixed in buffered

10% formalin overnight, embedded in paraffin sections with 5 μ thickness and prepared and stained with hematoxylin & eosin (H&E), and IHC detection of inducible nitric oxide synthase (iNOS). iNOS rabbit polyclonal antibody (Thermo Fisher scientific, Anatomical pathology, Tudor Road, Manor Park, Runcorn, Cheshire WA7 1TA, UK (7.0 mL) was used for reactive oxygen species (ROS) identification with brown cytoplasmic expression. In contrast, the remaining was prepared for polymerase chain reaction (PCR) examination. The slides were examined and photographed under a light microscope (Leica DM 1000, Danaher Corporation, United States) [11].

The assessment of the expression of iNOS involved determining the proportion of cells with positive immunostaining per 100 cells in 10 fields for each group. Image analysis was performed using Image J (1.46a, NIH, USA) software.

2.3. Quantitative real-time PCR (RT-Qpcr)

Analysis of heme oxygenase-1 (*HO-1*) gene expression using quantitative RT-qPCR was performed using RT-qPCR to evaluate levels of ROS. Tissue homogenization was performed using the Tissue Ruptor II (Qiagen, Hilden, Germany) in the presence of lysis buffer for 15–90 seconds. Then, the mixture was centrifuged at 4000 rpm for 20 minutes. Finally, the cell supernatant was collected for RNA extraction [12]. Then, RNA extraction and purification were performed using the RNeasy Mini kit (Qiagen, Hilden, Germany). After that, the reverse transcription step was performed by the QuantiTect Reverse Transcription Kit (Qiagen, Hilden, Germany), and the *HO-1* gene expression level was amplified using QuantiTect primer assay and QuantiTect SYBR Green PCR Kit (Qiagen, Germany). Relative changes in gene expression between two compared sequences were calculated using the $2^{-\Delta\Delta C_t}$ method [13].

2.4. Statistical analysis

All data were calculated, tabulated, and statistically analyzed using the computer program SPSS software, version 25.0 for Windows (Statistical Package for Social Science, Armonk, NY: IBM Corp) at significant levels 0.05 ($P < 0.05$). One-way analysis of variance (ANOVA) was used to compare data across groups, followed by Tukey's post hoc test was performed to evaluate statistical significance among them. Data were expressed as Mean \pm SD and range (Max-Min); the value of $P < 0.05$ was considered statistically significant. Independent student's t-test was performed to compare the mean differences between the two materials at the same method at $P < 0.05$.

3. Results

3.1. Histological findings

Histological results revealed regular histological features of the parenchymal element and connective tissue (CT) stroma in the control group. In the AA group, the serous acini (A) had ill-defined outlines and pyknotic and crescent-shaped nuclei with different-sized cytoplasmic vacuolations. Striated duct (S) cells showed signs of degeneration and loss of normal cell lining, basal striations, cell height with the presence of cytoplasmic vacuolation within the cells. Granular convoluted tubules (GCTs) showed cytoplasmic vacuolations with a marked decrease in granularity and eosinophilia. On the other hand, the NS group showed SMG regained their normal appearance. However, the minimum degree of atrophic changes among the acini and ducts were encountered in some regions. Serous acini lined by pyramidal-shaped cells with well-defined cell boundaries and apparently fewer cytoplasmic vacuolations were observed. The Ss showed an almost normal cell lining maintaining their normal basal striations with few cytoplasmic vacuolations, while GCTs presented signs of degeneration (Figure 1).

3.2. IHC expression of iNOS

The control group showed a very weak to mild immunoreactivity for iNOS among all glandular elements, which slightly increased in the duct system compared to the acinar portions. The AA group revealed a marked increase in the cytoplasmic iNOS immunoexpression throughout the SMG's parenchyma. The acini showed moderate immunoreactivity, while the entire duct system revealed a strong immunostaining intensity. As for NS treated group, a markedly reduced iNOS immunoreactivity was detected throughout the whole glandular parenchyma, where the acini reacted to iNOS weakly and the duct system presented a mild immunoreaction to iNOS (Figure 2).

Image analysis revealed that the AA group recorded the highest mean area % of iNOS immunoexpression, while the control group recorded the lowest, and a statistically significant difference was observed among all studied groups ($P < 0.05$). A highly significant increase in the mean area % of iNOS immunoexpression ($P < 0.0001$) was recorded in the by the AA group compared to the control group. Meanwhile, there was a non-significant increase in iNOS immunoexpression in the AA+NS group compared to the control group ($P = 0.0757$). Furthermore, a highly significant decrease in the mean area

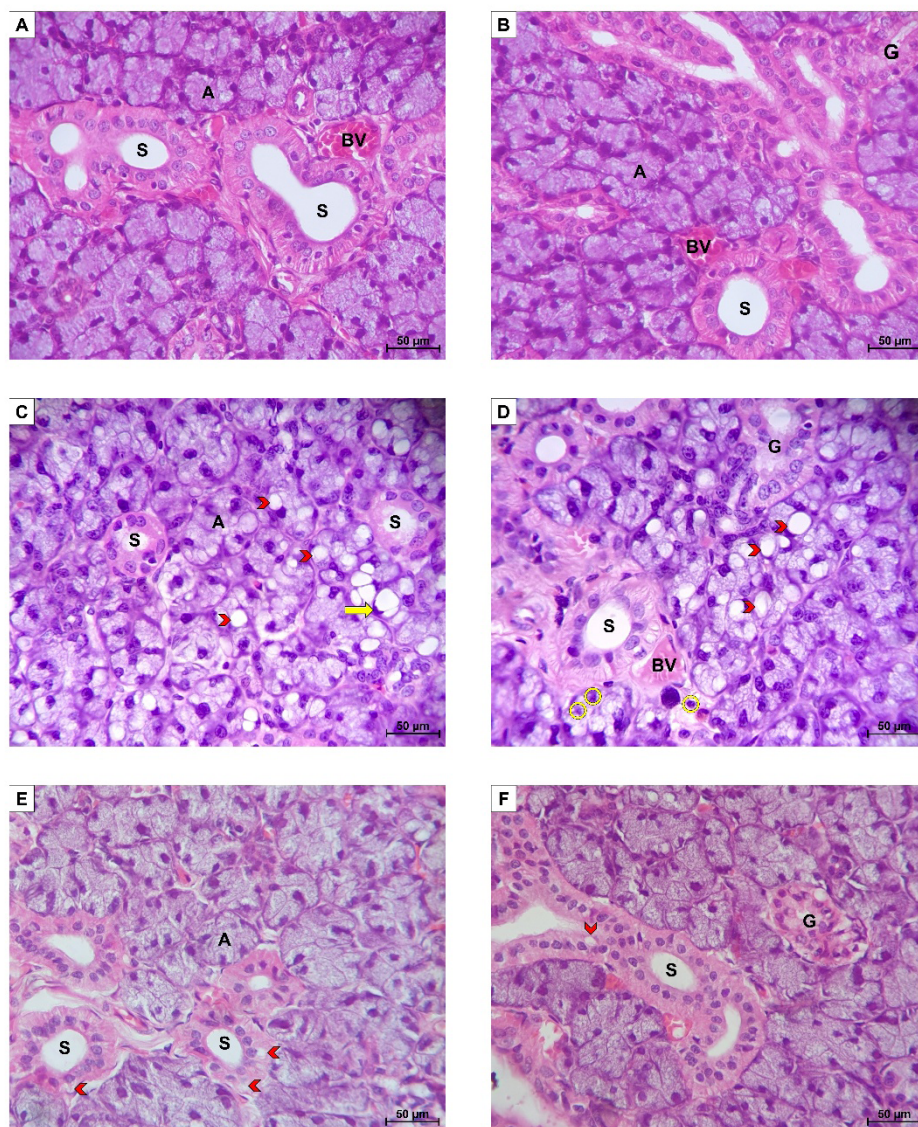


Figure 1. H&E section of SMG of albino rats

A and B) The control group showed normal gland architecture; C and D) AA group showing serous acini (A) with ill-defined outline (A) and crescent-shaped nuclei (arrow), pyknotic nuclei (yellow circle) and different-sized cytoplasmic vacuolations (arrow heads). GCTs (G) with cytoplasmic vacuolations and marked decrease in their granularity and eosinophilia as well as S with loss of normal cell lining, basal striations and different-sized cytoplasmic vacuolations associated with congested BV were also observed; E, F) NS group showed serous A with well-defined cell boundaries and apparently less cytoplasmic vacuolations, S maintaining their normal basal striations with few cytoplasmic vacuolations (arrow heads) and G showing signs of degeneration (H&E original magnification $\times 400$)

Abbreviations: A: Acini; S: Striated duct; G: GCTs; BV: Blood vessel.

% of iNOS immunoexpression was recorded by comparing the AA+NS group to the AA group ($P < 0.0001$) (Figure 3).

3.3. RT-PCR

The highest mean *HO-1* gene expression was recorded in the AA group. In contrast, the lowest was recorded in the control

group, and a statistically significant difference was observed among the whole studied groups ($P < 0.05$). Tukey's post hoc pairwise comparison revealed a highly significant increase in the mean *HO-1* gene expression in the AA group and AA+NS group compared to the control group ($P < 0.0001$). On the other hand, a significant decrease in the mean *HO-1* gene expression was recorded when comparing the AA+NS group to the AA group ($P < 0.001$) (Figure 4).

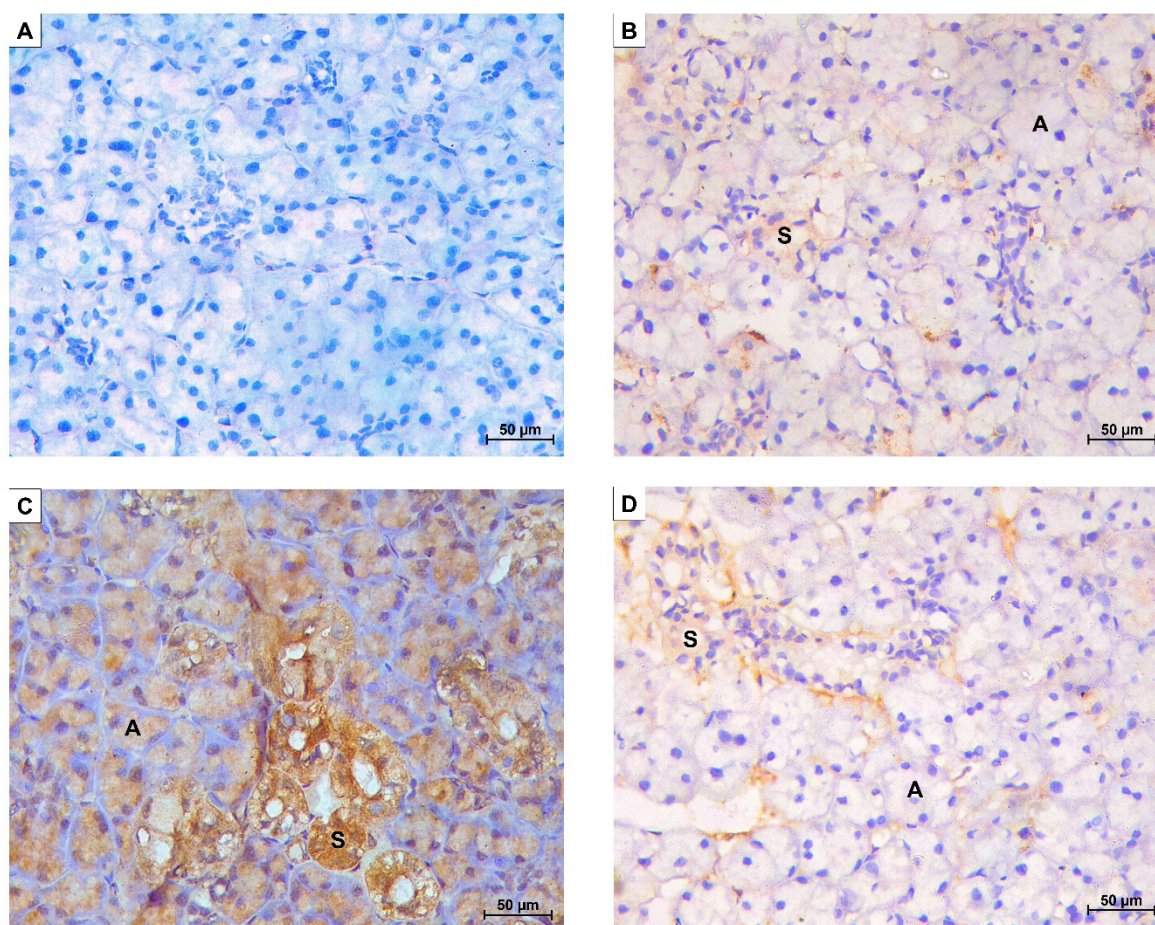


Figure 2. An immunostained section of iNOS antibody albino rats' SMG

A) Photomicrograph of the control group incubated with non-specific serum and color developed by DAP showing negative staining reaction of all the gland component; B) Control group showing weak to mild immunoreactivity to iNOS; C) AA group showed moderate immunoreactivity to iNOS in the A, while the entire duct system revealed a strong immunostaining intensity (S); D) NS group showed weak reaction to iNOS in the A and a mild immunoreaction in the S (original magnification $\times 400$)

Abbreviations: A: Acini; S: Striated duct; G: GCTs.

4. Discussion

AA is an unsaturated amide with high chemical activity, widely used in chemical industries and various consumer products. Owing to its various exposure routes, small molecular size, and high-water solubility, facilitating its rapid absorption and distribution throughout the body, AA toxicity has been thoroughly studied on human and experimental animals on different organs and systems. Given that dietary intake is considered the key source of AA exposure in humans [3], it only seemed logical that oral administration was selected as the route of choice in this study. AA dose was chosen based on the findings where it induced chronic AA toxicity in the parotid gland of albino rats. Furthermore, the selected dose is safely below the lethal dose (LD_{50}) for AA in rats, which is 150 mg/kg bw [14].

In the present study, histological examination of the SMG of the AA group showed marked signs of degeneration in the parenchymal elements of the gland, indicating AA's cytotoxic effect on the acinar and ductal cells. Similar degenerative changes in the acini and ducts of SMG were observed in another study following AA exposure [5]. Moreover, the same dose and duration of AA used in our study resulted in degenerative changes in the parotid gland architecture [15]. Both studies attributed these degenerative processes to AA generating excessive oxidative stresses, leading to mitochondrial dysfunction.

Excessive oxidative stress production, in turn, impairs mitochondrial function, which is crucial for energy production and cell survival, resulting in mitochondrial membrane damage and a decline in the Bcl-2/Bax ratio, initiating the intrinsic apoptotic pathway, causing

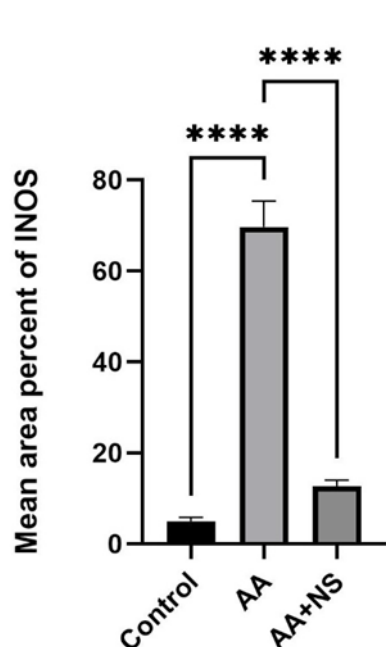


Figure 3. Bar chart of Mean \pm SD of iNOS mean area percent expression within experimental groups

****Statically significant ($P < 0.0001$).

cell death [16]. Additionally, mitochondrial dysfunction impairs cellular metabolic processes, such as glycolysis and respiration, exacerbating oxidative damage. The observed histological changes in this study in the acini as well as the loss of basal striations in the striated ducts can be directly linked to AA-induced oxidative stress and mitochondrial dysfunction. Accumulation of oxidative stresses leads to mitochondrial degeneration and loss of basal infoldings, due to AA toxicity [5]. This unified mechanism of damage aligns with previous studies, further highlighting the role of ROS in AA toxicity [16, 17]. Moreover, the current results are consistent with the findings of Liu et al. [17], who concluded that AA hinders cell metabolic activity by suppressing the expression of complex I, III, and IV subunits and anaerobic glycolysis and mitochondrial respiration.

Different-sized cytoplasmic vacuolations observed histologically in the acinar and ductal cells in the experimental groups were consistent with other studies investigating AA toxicity on submandibular and parotid salivary glands [5, 15]. According to Hamza et al. [18] in cases of high oxidative stress and lipid peroxidation (LPO), vacuolization reflects cellular swelling, where the failure of the energy-dependent Na^+ - K^+ ion pumps in the plasma membranes occurs. Consequently, this leads to intracellular accumulation of Na^+ and gradual osmolarity shifts, allowing water to enter into the cells.

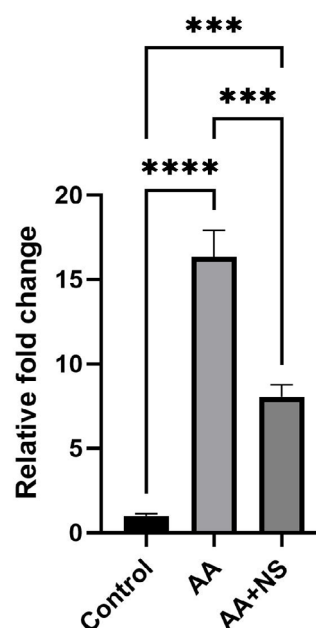


Figure 4. Bar chart of Mean \pm SD of *HO-1* expression within experimental groups

and * Statically significant ($P < 0.001$, $P < 0.0001$).

Nitric oxide synthases (NOSs) are a class of enzymes that convert L-arginine to L-citrulline, resulting in the formation of NO, a free radical and essential cellular signaling molecule. iNOS, an isoform of NOS, is produced only when a cell is activated or triggered, usually by proinflammatory cytokines and/or bacterial lipopolysaccharides [19]. Moreover, several studies demonstrated an increase in iNOS expression in cases of oxidative stress, leading to NO generation [19]. This may explain the elevation in iNOS immunorexpression noted in the AA group, which supports the hypothesis that the cytotoxic damage may indicate an inflammatory process and oxidative stress. On the other hand, *HO-1* is an inducible enzyme triggered by oxidative stress, catalyzing heme degradation and preventing apoptosis in response to proinflammatory agonists, thereby minimizing the detrimental effects of inflammation. The up-surge of *HO-1* gene expression in the AA group also aligns with Facchinetti [20], who reported elevated ROS or inflammatory mediators could account for increased *HO-1* expression. Moreover, *HO-1* expression is usually minimal or nonexistent under homeostatic conditions but is dramatically upregulated in response to pro-oxidant stimuli, protecting against oxidative damage [21].

This research chose NS oil as a protective dietary component against AA toxicity, due the reported antioxidant, anti-apoptotic, anti-inflammatory, antiviral, and immunomodulatory activities. The selected dose has been

reportedly effective in upgrading oxidative stress damage in different brain regions of rats, including the cerebellum, cortex, and hippocampus [10]. In the present study, NS oil intake demonstrated a cytoprotective effect against the harmful impact of AA on the SMG of rats, as evidenced by histological and IHC analysis and molecular analysis. This agrees with several studies, investigating NS oil's effect on oxidative stress-induced toxicity in different tissues [22]. This cytoprotective effect of NS oil can be attributed to its anti-apoptotic, anti-oxidative, and anti-inflammatory properties, which was evident by a significant down-regulation of iNOS immunoeexpression and *HO-1* gene expression. It was reported that NS supplementation significantly increased antioxidant enzyme levels (GSH and SOD), reduced LPO levels, and down-regulated pro-inflammatory mediators following AA-induced oxidative stress [23]. Studies have also reported the ability of NS to down-regulate iNOS immunoeexpression, inhibiting NO production and highlighting its powerful antioxidant ability [24, 25]. Moreover, studies have confirmed the capacity of NS oil to mitigate oxidative stresses and inflammation through a dose-dependent inhibition in *HO-1* gene expression after NS oil administration [26, 27].

AA administration has a cytotoxic effect on the parenchymal element of SMG due to excessive production of oxidative stress. NS oil treatment exerted an apparent therapeutic effect against AA-induced toxicity on SMG making. It is a promising candidate to combat oxidative stress, inflammation, and apoptosis.

Ethical Considerations

Compliance with ethical guidelines

This research was approved by the Research Ethics Committee (REC) of the Faculty of Dentistry, Suez Canal University, Ismailia, Egypt (Code: 474/2022), in accordance with institutional guidelines for animal experimentation.

Data availability

The data used and/or analyzed during the current study are available from the corresponding author upon reasonable request

Funding

This research did not receive any grant from funding agencies in the public, commercial, or non-profit sectors.

Authors' contributions

Conceptualization and study design: Salma Awad Taghyan and Elham Fathy Mahmoud; Data analysis and interpretation: Rasha Mohamed Taha and Mohamed Shamel; Investigation: Salma Awad Taghyan and Mohamed Shamel; Writing the original draft: Salma Awad Taghyan; Review and editing: Elham Fathy Mahmoud, Rasha Mohamed Taha, and Mohamed Shamel; Supervision: Elham Fathy Mahmoud.

Conflict of interest

The authors declared no conflict of interest.

Acknowledgements

The authors express their gratitude to everyone who contributed to the completion of this study.

References

- [1] Elhelaly AE, Albasher G, Alfarraj S, Almeer R, Bahbah EI, Fouda MM, et al. Protective effects of hesperidin and diosmin against acrylamide-induced liver, kidney, and brain oxidative damage in rats. *Environ Sci Pollut Res Int*. 2019; 26(34):35151-62. [DOI:10.1007/s11356-019-06660-3] [PMID]
- [2] Dahrhan N, Abd-Elhakim YM, Mohamed AA, Abd-Elsalam MM, Said EN, Metwally MM, et al. Palliative effect of Moringa olifera-mediated zinc oxide nanoparticles against acrylamide-induced neurotoxicity in rats. *Food Chem Toxicol*. 2023; 171:113537. [DOI:10.1016/j.fct.2022.113537] [PMID]
- [3] Zhao M, Zhang B, Deng L. The mechanism of acrylamide-induced neurotoxicity: Current status and future perspectives. *Front Nutr*. 2022; 9:859189. [DOI:10.3389/fnut.2022.859189] [PMID]
- [4] Abdel-Daim MM, Abo El-Ela FI, Alshahrani FK, Bin-Jumah M, Al-Zharani M, Almutairi B, et al. Protective effects of thymoquinone against acrylamide-induced liver, kidney and brain oxidative damage in rats. *Environ Sci Pollut Res*. 2020; 27:37709-17. [DOI:10.1007/s11356-020-09516-3]
- [5] Mahmoud EF, Zahran DH, Mahmoud MF. Histological, immunohistochemical and ultrastructural evaluation of the cytotoxic effect of acrylamide on submandibular salivary glands in rats. *Dent Journal*. 2013; 59(4):3775-85. [Link]
- [6] Al-Serwi RH, Ghoneim FM. The impact of vitamin E against acrylamide induced toxicity on skeletal muscles of adult male albino rat tongue: Light and electron microscopic study. *J Microsc Ultrastruct*. 2015; 3(3):137-47. [DOI:10.1016/j.jmau.2015.03.001] [PMID]

- [7] Amin B, Hosseinzadeh H. Black cumin (*Nigella sativa*) and its active constituent, thymoquinone: An overview on the analgesic and anti-inflammatory effects. *Planta Med.* 2016; 82(1-2):8-16. [DOI:10.1055/s-0035-1557838] [PMID]
- [8] Hannan MA, Rahman MA, Sohag AAM, Uddin MJ, Dash R, Sikder MH, et al. Black cumin (*Nigella sativa* L.): A comprehensive review on phytochemistry, health benefits, molecular pharmacology, and safety. *Nutrients.* 2021; 13(6):1784. [DOI:10.3390/nu13061784] [PMID]
- [9] Faul F, Erdfelder E, Buchner A, Lang AG. Statistical power analyses using G* Power 3.1: Tests for correlation and regression analyses. *Behav Res Methods.* 2009; 41(4):1149-60. [DOI:10.3758/BRM.41.4.1149] [PMID]
- [10] Mohamadin AM, Sheikh B, Abd El-Aal AA, Elberry AA, Al-Abbasi FA. Protective effects of *Nigella sativa* oil on propoxur-induced toxicity and oxidative stress in rat brain regions. *Pestici Biochem Physiol.* 2010; 98(1):128-34. [DOI:10.1016/j.pestbp.2010.05.011]
- [11] Shamel M, Baz S, Mahmoud H, Taghyan SA, Bakr MM, Al Ankily M. Balancing Risks versus Benefits: Vitamin C Therapy versus Copper Oxide Nanoparticles Toxicity in Albino Rats' Submandibular Salivary Gland. *Eur J Dent.* 2025; 19(1):124-32. [DOI:10.1055/s-0044-1786867] [PMID]
- [12] Sparmann G, Jäschke A, Loehr M, Liebe S, Emmrich J. Tissue homogenization as a key step in extracting RNA from human and rat pancreatic tissue. *Biotechniques.* 1997; 22(3):408-12. [DOI:10.2144/97223bm07] [PMID]
- [13] Livak KJ, Schmittgen TD. Analysis of relative gene expression data using real-time quantitative PCR and the 2- $\Delta\Delta CT$ method. *Methods.* 2001; 25(4):402-8. [DOI:10.1006/meth.2001.1262] [PMID]
- [14] Elswawi NM, Abo Kresha SAT, Mohamed MA, Khorshed A, Aldajani W, Rajeh NA, et al. Curcumin Ameliorates Acrylamide Induced Ovarian Toxicity in Albino Female Rats: A Biochemical and Histological Study. *Egypt J Chem.* 2023; 66(3):157-68. [DOI:10.21608/ejchem.2022.139554.6136]
- [15] Al-Serwi RH, Anees MM, Abd Elhamied AS. Biological effect of acrylamide on parotid salivary gland of Albino rats. *Egypt Dent J.* 2016; 62(1):37-45. [Link]
- [16] Bakr MM, Al-Ankily MM, Shogaa SM, Shamel M. Attenuating effect of vitamin E against Silver Nano Particles Toxicity in Submandibular Salivary Glands. *Bioengineering.* 2021; 8(12):219. [DOI:10.3390/bioengineering8120219] [PMID]
- [17] Liu Z, Song G, Zou C, Liu G, Wu W, Yuan T, et al. Acrylamide induces mitochondrial dysfunction and apoptosis in BV-2 microglial cells. *Free Radic Biol Med.* 2015; 84:42-53. [DOI:10.1016/j.freeradbiomed.2015.03.013] [PMID]
- [18] Hamza SA, Aly HM, Soliman SO, Abdallah DM. Ultrastructural study of the effect of zinc oxide nanoparticles on rat parotid salivary glands and the protective role of quercetin. *Alex Dent J.* 2016; 41(3):232-7. [DOI:10.21608/alexu.2016.58053]
- [19] Cinelli MA, Do HT, Miley GP, Silverman RB. Inducible nitric oxide synthase: Regulation, structure, and inhibition. *Med Res Rev.* 2020; 40(1):158-89. [DOI:10.1002/med.21599] [PMID]
- [20] Facchinetti MM. Heme-Oxygenase-1. *Antioxid Redox Signal.* 2020; 32(17):1239-42. [DOI:10.1089/ars.2020.8065] [PMID]
- [21] Campbell NK, Fitzgerald HK, Dunne A. Regulation of inflammation by the antioxidant haem oxygenase 1. *Nat Rev Immunol.* 2021; 21(7):411-25. [DOI:10.1038/s41577-020-00491-x] [PMID]
- [22] Ayuob NN. Histological and immunohistochemical study on the possible ameliorating effects of thymoquinone on the salivary glands of rats with experimentally induced hypothyroidism. *Egypt J Histol.* 2016; 39(2):125-35. [DOI:10.1097/01.EHX.0000489145.55478.51]
- [23] Hatipoğlu D, Özsan M, Dönmez HH, Dönmez N. Hepatoprotective effects of *nigella sativa* oil against acrylamide-induced liver injury in rats. *Ankara Üniv Vet Fak Derg.* 2023; 70(4):1-22. [DOI:10.33988/auvfd.1096306]
- [24] Fathy M, Nikaido T. In vivo modulation of iNOS pathway in hepatocellular carcinoma by *Nigella sativa*. *Environ Health Prev Med.* 2013; 18(5):377-85. [DOI:10.1007/s12199-013-0336-8] [PMID]
- [25] Montazeri RS, Fatahi S, Sohoul M, Abu-Zaid A, Santos HO, Gâman MA, et al. The effect of *nigella sativa* on biomarkers of inflammation and oxidative stress: A systematic review and meta-analysis of randomized controlled trials. *J Food Biochem.* 2021; 45(4):e13625. [DOI:10.1111/jfbc.13625] [PMID]
- [26] Ahmad A, Alkharfy KM, Jan BL, Ahad A, Ansari MA, Al-Jenoobi FI, et al. Thymoquinone treatment modulates the Nrf2/HO-1 signaling pathway and abrogates the inflammatory response in an animal model of lung fibrosis. *Exp Lung Res.* 2020; 46(3-4):53-63. [DOI:10.1080/01902148.2020.1726529] [PMID]
- [27] Salim EI. Gene profiling cDNA microarray analysis of rat colon carcinogenesis treated with crude *nigella sativa* oil. *Egypt J Exp Biol (Zool.).* 2015; 7(2):213-21. [Link]